Article published online: 2021-07-30

Imaging of lung cancer: Implications on staging and management

Nilendu C Purandare, Venkatesh Rangarajan

Department of Nuclear Medicine and Molecular Imaging, Tata Memorial Hospital, Mumbai, Maharashtra, India

Correspondence: Dr. Nilendu C Purandare, Department of Nuclear Medicine and Molecular Imaging, Tata Memorial Hospital, Parel, Mumbai - 400 012, Maharashtra, India. E-mail: nilpurandare@gmail.com

Abstract

Lung cancer is one of the leading causes of cancer-related deaths. Accurate assessment of disease extent is important in deciding the optimal treatment approach. To play an important role in the multidisciplinary management of lung cancer patients, it is necessary that the radiologist understands the principles of staging and the implications of radiological findings on the various staging descriptors and eventual treatment decisions.

Key words: Computed Tomography scan; imaging; lung cancer; Positron emission tomography-computed tomography; staging

Introduction

Lung cancer is the leading cause of cancer-related deaths for both men and women across the developed world. Despite tremendous efforts to treat this cancer, the overall 5-year survival for all stages is dismally low at 15%,[1] since most patients present at an advanced stage when curative treatment is no longer an option. Even in India, though the incidence of oral, breast, and cervix cancer is higher, lung cancer accounts for the highest number of cancer deaths among men.[2] Though majority of patients present at an advanced stage, those with early-stage lung cancer can be treated with a potentially curative intent. Thus, the importance of early diagnosis as well as appropriate radiological staging cannot be overemphasized. In this review, various typical and atypical radiological patterns of lung cancer are depicted and various imaging issues which are relevant for appropriate staging are discussed. Imaging findings and their implications on treatment decisions are also included in this article.

Access this article online	
Quick Response Code:	Website: www.ijri.org
	DOI: 10.4103/0971-3026.155831

Imaging Appearance of Lung Cancer

Majority of the lung cancer patients (approx 80%) are clinically symptomatic and present with cough, hemoptysis, dyspnea, chest pain, and non-resolving pneumonia.[3] Occasionally, they present with features suggestive of metastatic disease like skeletal pain or neurological symptoms and signs. Less than 10% of the patients are asymptomatic when the cancer is detected as an incidental finding.[3] Lung cancer is classified as either non-small cell lung cancer (NSCLC) or small cell lung cancer, with the NSCLC accounting for the vast majority (87%).[4] Chest radiograph is the first investigation which is performed while investigating a suspected case of lung cancer. Though it is a very good tool in providing preliminary information about the disease, it is inadequate for optimal characterization and staging. Computed Tomography (CT) scan of the chest is the cornerstone of lung cancer imaging based on which further management is decided. The primary tumor shows a wide spectrum of imaging appearances. NSCLCs can be centrally located masses, invading the mediastinal structures [Figure 1A], or peripherally situated lesions [Figure 1B] that invade the chest wall. Tumors can have margins which are smooth, lobulated [Figure 1C], or irregular and spiculated [Figure 1D]. They can be uniformly solid or can have central necrosis and cavitation [Figure 2A]. Centrally situated and cavitating tumors are more likely to be of squamous histology. Sometimes the tumor resembles an infective pathology

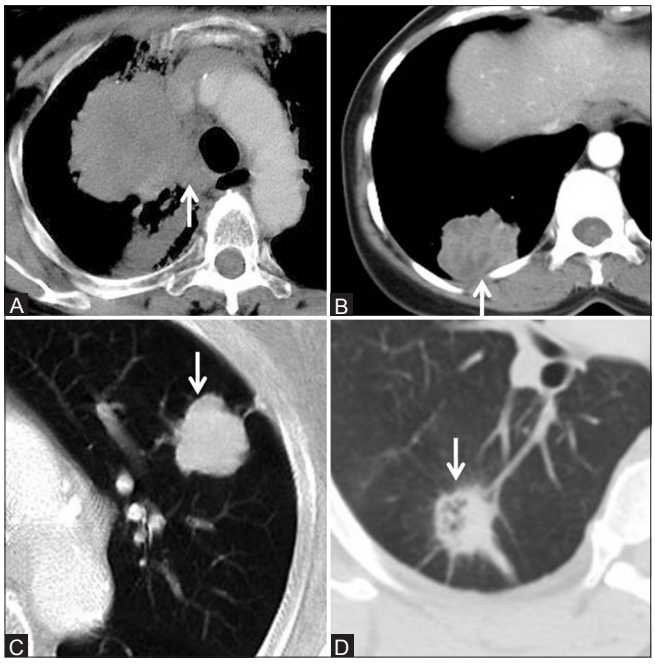

Figure 1 (A-D): Common radiological appearances of lung cancer. Centrally located mass with mediastinal invasion (arrow, A), peripherally situated mass abutting the pleura (arrow, B), mass with smooth, lobulated margins (arrow, C) and with spiculated, irregular margins (arrow, D)

and is seen as an area of consolidation [Figure 2B], a ground-glass opacity [Figure 2C, or a combination of both [Figure 2D]. Such an appearance is more commonly seen with adenocarcinoma and its subtypes. Mixed density or pure ground-glass nodules and consolidation with air bronchogram are seen in bronchoalveolar carcinomas, which are now referred to as adenocarcinoma *in situ* [Figure 2D]. Whatever the imaging appearance of the suspected lung cancer, obtaining tissue diagnosis by performing a bronchoscopic or an image-guided biopsy is necessary. When lung cancer is incidentally detected in an aymptomatic patient, it is often seen as a solitary pulmonary nodule (SPN) which can have varied imaging appearances. Imaging algorithm of SPN is a vast subject in itself and has not been included in this review.

Imaging Correlates of Recent TNM Staging

Currently the 7th edition of TNM staging is followed in clinical practice for lung cancer staging. Revisions in staging systems are based on recommendations by the International Association for Study of Lung Cancer (IASLC).[5] Changes to the staging system from 6th to 7th edition were intended to more accurately reflect the relationship between T (primary tumor), N (nodal involvement), and M (metastatic disease) descriptors with patient prognosis and survival. Though lung cancer staging has been described in greater detail later in this chapter, overall, stage I cancer is confined to the lungs, stage II refers to disease that involves the lungs and the ipsilateral hilar, peribronchial, and bronchopulmonary

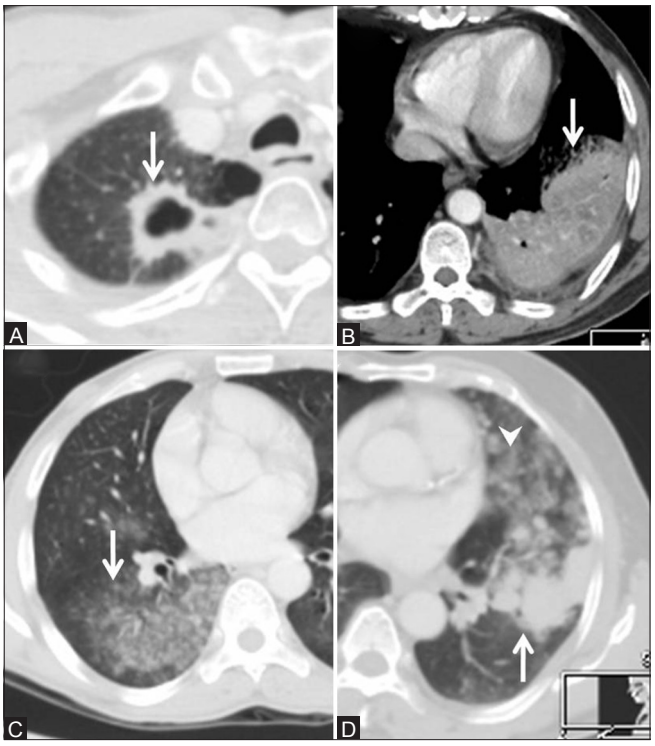

Figure 2 (A-D): Lung cancers with atypical radiological pattern. Squamous cell cancer presenting as a cavitating mass (arrow, A). Adenocarcinoma presenting as dense consolidation (arrow, B). Bronchoalveolar carcinoma (adenocarcinoma in situ) presenting as ground-glass opacity (arrow, C) and mixed density, solid (arrow), and ground-glass nodules (arrowhead) in D

nodes, stage IIIA refers to disease that has spread to ipsilateral mediastinal nodes or contiguously involving structures like chest wall and pericardium that can be resected, stage IIIB is non-resectable disease that involves contralateral mediastinal or supraclavicular nodes, and stage IV involves distant spread of disease.

T (tumor) descriptor

The extent of spread of the primary tumor is shown by the T descriptors which involve tumor size, invasion of adjacent structures, endobronchial location and distance from the carina, and presence of satellite nodules.

T1: Tumors that are less than 3 cm in size, surrounded by lung parenchyma/visceral pleura, and do not show invasion proximal to the lobar bronchus are classified as stage T1 tumors [Figure 3A]. As per the 7th edition, T1 tumors are further subdivided into T1a (≤2 cm) and T1b (>2 cm but ≤3 cm). The rationale for this subdivision was based on difference in survival. Patients with nodules described under T1a had a 5-year survival of 77%; by comparison, those qualifying as T1b had a 5-year survival of 71%.[6]

T2: Tumors with invasion of the visceral pleura, with atelectasis and obstructive pneumonitis extending to the hilar region but not involving the entire lung, are considered stage T2 tumors [Figure 3B]. It also included

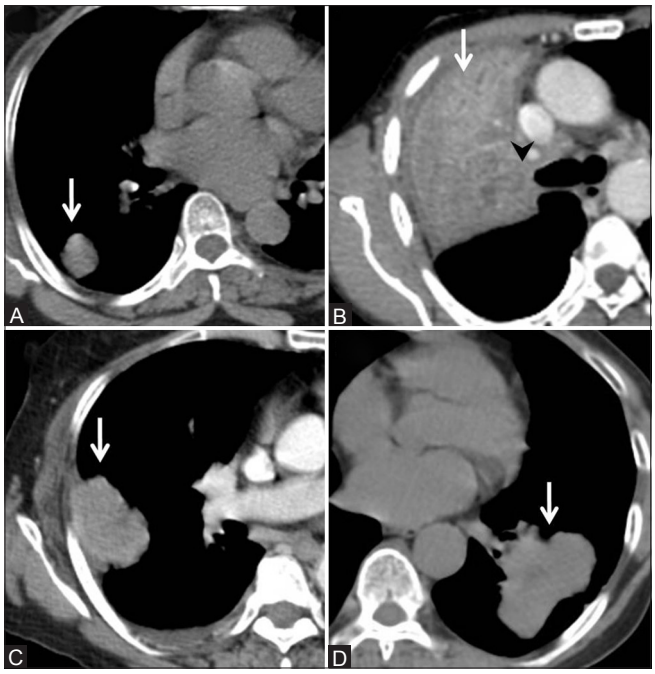

Figure 3 (A-D): Stage T1 and T2 tumors. Stage T1 tumor due to size <3 cm (arrow, A). Stage T2 endobronchial tumor (arrowhead) causing pneumonitis restricted to the upper lobe (arrow) in B. T2a tumor >3 cm but <5 cm (arrow, C). T2b tumor >5 cm but <7 cm (arrow in D)

endobronchial lesions situated more than 2 cm distal to the carina. T2 tumors are further subdivided into T2a (>3 cm but ≤5 cm) [Figure 3C] and T2b (>5 cm but ≤7 cm) [Figure 3D]. The rationale for this subdivision was also based on survival. Patients with tumors described under T2a had a 5-year survival of 58% and those classified as T2b had a 5-year survival of 49%.[6]

T3 and T4: Tumors larger than 7 cm in size are classified as stage T3 [Figure 4A]. Satellite nodule in the same lobe is also considered to be stage T3. Tumors with invasion of the chest wall [Figure 4B], diaphragm, mediastinal pleura [Figure 4C], parietal pericardium; tumors with atelectasis and obstructive pneumonitis affecting the entire lung [Figure 4D]; and endobronchial lesions less than 2 cm distal to the carina but not involving it are considered as T3 neoplasms. As per the previous classification, satellite nodule in the same lobe was regarded as T4 tumor. However, the 5-year survival of patients with satellite nodule in the same lobe was similar to other types of T3 tumors;[6] hence, in the recent classification, they are classified as T3 instead of T4. Previously, those tumors with an ipsilateral satellite nodule in a different lobe were classified as having metastatic disease (M1). However, such patients had a 5-year survival of 22%, which was identical to those with T4 disease due to other criteria.[6] Hence, tumors with satellite nodule in a different lobe of the same lung were reclassified as stage T4. Tumors that infiltrate the mediastinum, trachea, esophagus, recurrent laryngeal nerve, great vessels, vertebrae, and heart and endobronchial lesions that involve the carina are

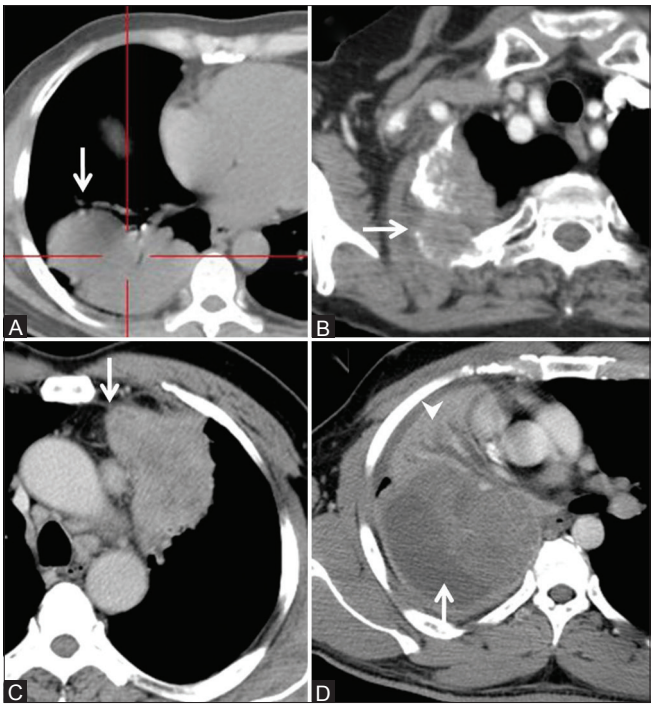

Figure 4 (A-D): Stage T3 tumors. T3 tumor due to size >7 cm in size (arrow, A), eroding the ribs (arrow, B), infiltrating the mediastinal pleura but not the vessels (arrow, C), and causing atelectasis of the entire lung (arrowhead, D)

considered to be stage T4 [Figure 5] and these descriptors remain unchanged between the previous and recent editions.

Imaging Modalities for T Stage and Implications of Radiological Findings On Treatment

Chest radiograph, CT scan, positron emission tomography (PET) scan, and Magnetic Resonance Imaging (MRI) are the modalities that can determine the T stage. Standard chest radiograph has a limited utility in T staging. Though it can demonstrate obvious chest wall and mediastinal invasion in large tumors, it has a limited sensitivity to predict T3 and T4 disease and patient has to undergo further imaging for better delineation of extent and resectability.

CT scan is the most commonly used imaging modality for T staging. T1, T2, T3, and some T4 tumors are considered to be technically resectable. Even if a tumor is classified as T1, certain relevant information needs to be conveyed to the surgeon, such as proximity of the tumor to the main pulmonary artery and whether it crosses the fissures, as surgical approaches may have to altered accordingly. Endobronchial tumor involvement and its distance from the carina is an important finding that can decide the surgical approach; however, surgeons tend to rely more on bronchoscopy findings under direct vision to evaluate endobronchial tumor extension.

Invasion of the chest wall does not preclude surgical excision; hence, its presence and extent needs to be conveyed as chest wall reconstructive procedures to close large defects have to be planned in addition to tumor excision. The reported sensitivity of CT scan for chest wall invasion varies from 38 to 87% and the specificity varies from 40 to 90%.[7] Likewise, MRI also shows a wide range of sensitivity (63-90%) with a specificity of 84-86%.[8,9] Findings such as abutment or large area of contact of the tumor with the ribs and scalloping are at the best suggestive but not diagnostic of chest wall invasion. More definitive findings of invasion are lysis/destruction or definite sclerosis of ribs, and tumor soft tissue in the chest wall musculature [Figure 5]. According to one study, local pain was more sensitive and accurate than CT scan in predicting chest wall invasion.[10]

Mediastinal invasion is an important finding in deciding resectability. Tumoral invasion of the mediastinal pleura and the fatty tissue is classified as stage T3 and it does not preclude resection [Figure 4C]. However, infiltration of the mediastinal great vessels, esophagus, trachea, and vertebral body is staged as T4 and makes the tumor unresectable [Figure 5]. Findings on CT scan like obliteration of fat plane between the tumor and the mediastinum, circumference of contact between the tumor and the aorta, and the length of anatomical contact between the tumor and the mediastinum are not definitive signs for invasion. Both CT scan and MRI have similar diagnostic accuracy (56-89% for CT and 50-93% for MRI) in predicting mediastinal invasion, with no modality being considered to be distinctly superior. Patients with operable tumors often undergo quantitative lung perfusion scintigraphy for pre-operative assessment of lung function to identify those who are at increased risk of having peri-operative complications and long-term disability due to surgical resection of the lung.

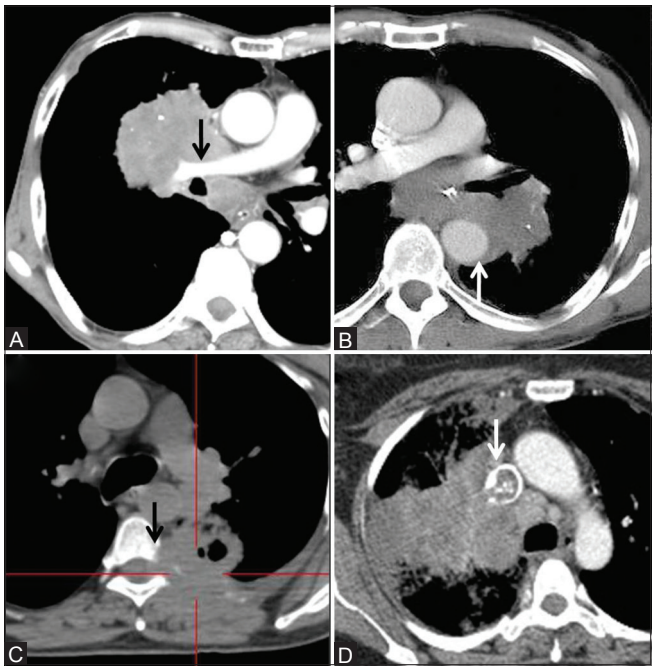

Figure 5 (A-D): Stage T4 tumors. T4 tumor due to invasion of pulmonary artery (arrow, A), descending aorta (arrow, B), vertebral body (arrow, C), superior vena cava with thrombus (arrow, D)

Role of FDG PET/CT for T stage

CT scan is the modality of choice and can provide all the necessary information needed for T staging. On its own, the fludeoxyglucose (18F) (FDG) PET component of the study does not have the optimal spatial resolution to provide information about infiltration of adjacent structures and, thus, has limitations for T staging. However, if FDG PET is performed along with contrast-enhanced CT, then the integrated imaging study has a similar accuracy as CT scan. Occasionally, it is difficult to determine the exact tumor location and extent on CT scan due to surrounding atelectasis. In such situations, FDG PET/CT can accurately delineate the viable tumor from surrounding atelectasis and collapse/consolidation [Figure 6]. This information can not only demarcate the size and extent of the tumor for accurate T staging[11] but also provide guidance for biopsies if histological confirmation is required or prior biopsy attempts have led to inconclusive pathological results[12] [Figure 6].

N (nodal) descriptor

Accurate N staging is an important prognostic factor and is critical in deciding the best treatment option. Two systems for nodal mapping have been used over the years: One proposed by the American Thoracic Society (ATS) surgeons using the Mountain–Dressler system and other by Japanese surgeons using the Naruke classification.[13,14] The use of two different systems leads to confusion and difficulty in performing statistical analysis for nodal disease. The IASLC has proposed a new system which has a unified and simplified approach to nodal mapping. The details for this new IASLC system of nodal maps can be accessed from the article by Lusch *et al*.[15] [Figure 7]. Nodes in the hilar,

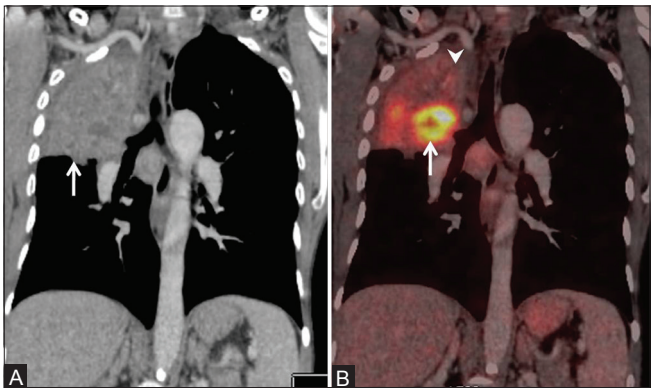

Figure 6 (A and B): Role of FDG PET/CT in primary tumor delineation. Irregular soft tissue opacity seen on coronal CT scan (arrow, A) with no obvious demarcation between the tumor and surrounding consolidation. PET/CT shows the FDG-avid tumor (arrow, B) separate from the non–FDG-avid consolidation (arrowhead, B)

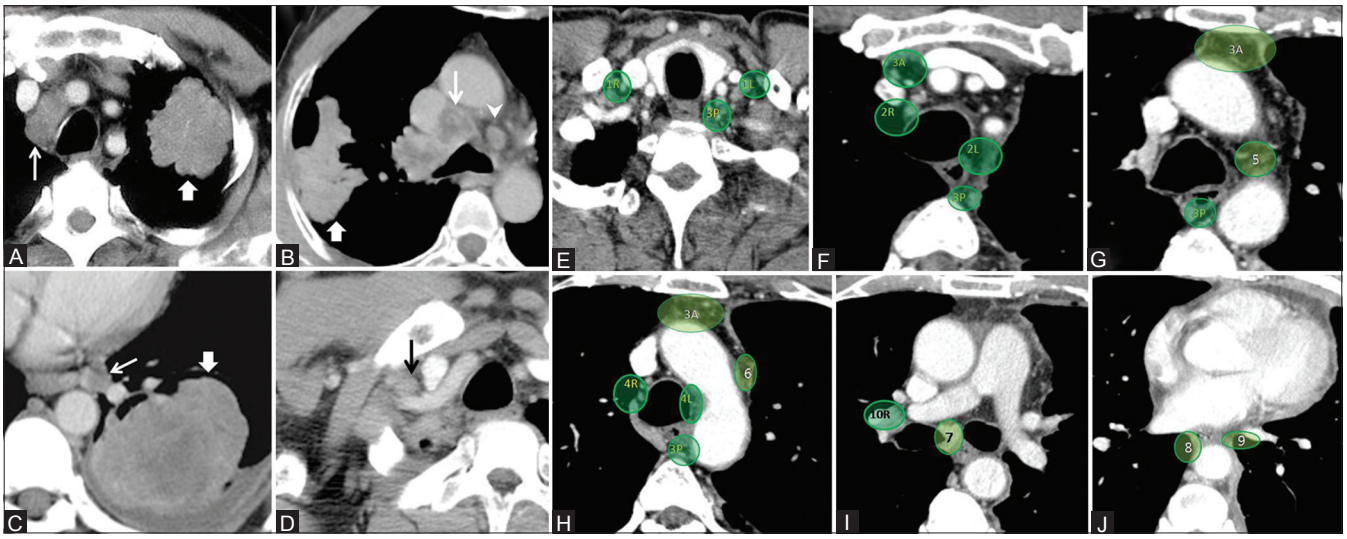

Figure 7 (A-J): (A-D) Nodal disease. Right upper paratracheal nodes-N3 (arrow, 7A) in a left-sided lung cancer (block arrow, A). Pretracheal-N2 (arrow, B) and aortopulmonary-N3 (arrowhead, B) nodes in a right-sided lung cancer (block arrow, B). Left inferior pulmonary ligament node-N2 (arrow, C) in a left-sided lung cancer (block arrow, C). Right scalene node-N3 (arrow, D). (E-J) Nodal stations. Nodal stations based on the IASLC map (ref 15). Station 1 (E)- Low cervical, supraclavicular, and sternal notch; station 2 (E and F)- upper paratracheal; station 3a (F-H)- prevascular; station 3p (F-H)- retrotracheal; station 4 (H)- lower paratracheal; station 5 (G)- aortopulmonary window; station 6 (H)- para-aortic (ascending aorta or phrenic); station 7 (I)- subcarinal; station 8 (J)- paraesophageal (below carina); station 9 (J)- pulmonary ligament; station 10 (I)- hilar; stations 11-14 are not included in the figure

interlobar, lobar, segmental, and subsegmental regions are referred as N1 disease. Ipsilateral mediastinal nodes are considered as N2 disease and it includes nodes in the upper paratracheal, prevascular and retrotracheal, lower paratracheal, subcarinal, paraesophageal, and pulmonary ligament regions [Figure 7]. Involvement of ipsilateral or contralateral supraclavicular lymph nodes or extension to nodes in the contralateral mediastinal, hilar/interlobar, or peripheral zones is classified as N3 disease [Figure 7]. One of the important changes introduced in the new IASLC map is the shifting of boundary between the right and left sides of the mediastinum to the left lateral border of the trachea, instead of the midline division of the trachea proposed by the ATS. Unlike for T stage where there was subdivision and reclassification of T descriptors based on survival curves, the N descriptors have not changed in the current 7th edition as there was no overlap of survival curves and the survival progressively worsened with increasing N stage.[5]

Imaging Modalities for N Stage and Implications of Radiological Findings on Treatment

The presence of mediastinal adenopathy is crucial in deciding resectability of the disease. Hilar, lobar, and interlobar nodes (N1 disease) and ipsilateral mediastinal or subcarinal adenopathy (N2 disease) may be resectable [Table 1]. However, contralateral mediastinal adenopathy or any scalene or supraclavicular adenopathy constitutes N3 disease, which is considered to be inoperable. It is important to describe the location and extent of N2 disease, since these patients are treated with neo-adjuvant chemotherapy followed by definitive surgical resection[16] [Table 1]. However, if the N2 disease is bulky and involves multiple nodal stations, then a combination of chemotherapy and radiotherapy might be preferred over surgery. In case of N3 disease, the treatment is mainly non-surgical, and if the patient has a good performance status, then he is treated with concurrent chemo-radiation therapy[17] [Table 1]. The exact description of the location and extent of adenopathy is important as it helps the radiation oncologist plan his radiation portals. If mediastinal nodal disease is extensive, radiation fields might become too large increasing the risk of radiation toxicity; in such a scenario, radical chemo-radiation therapy might be deferred and patients are treated with palliative chemotherapy instead.

Mediastinal nodal disease is evaluated using CT scan and more recently, PET/CT has been used for its evaluation. Size of the lymph node is the criterion used on CT scan to distinguish benign from malignant nodes. A node with short axis diameter of more than 1 cm is generally considered to be malignant. The use of size cut-off is inherently an erroneous approach as inflammatory nodes which are larger than 1 cm will be called as malignant and cancerous nodes smaller than 1 cm will be called as benign. Owing to this limitation, CT scan is not considered the optimal modality to evaluate mediastinal nodal disease, with reported combined sensitivity of 60-83%, specificity of 77-82%, and accuracy of 75-80% as per two meta-analyses.[18,19] Some have tried to using short axis diameter of 1.3 cm as the cut-off instead of 1.0 cm in order to reduce the false positives, leading to an improvement of specificity to 94% and accuracy to 86% for N2 disease.[20] Even with the development of multi-detector

CT technology with isotropic imaging and better resolution, there is no further improvement in the ability of CT scan to accurately stage the mediastinum.

Role of FDG PET/CT for N stage

With the increasing use of FDG PET in staging of lung cancer, improvement in diagnostic accuracy of imaging for mediastinal nodal disease has been documented. This was primarily because of the rationale that FDG PET can differentiate hyperplastic/reactive nodes from metastatic nodes and is used in the detection of metastasis within normal-sized nodes [Figure 8]. Even in the early days of the use of FDG PET, studies have shown better nodal staging accuracy for PET as compared to CT, with a sensitivity of 79% and specificity of 91% for PET compared with 60% and 77%, respectively, for CT.[19] A recent meta-analysis, the largest till date on FDG PET in lung cancer which included 56 studies and approximately 8700 patients, showed a pooled sensitivity of 72% and specificity of 91% for mediastinal nodal disease.[21] Despite the high diagnostic accuracy of FDG PET for mediastinal nodal disease reported in literature, the clinically relevant question remains whether a negative FDG PET study can obviate the need for invasive nodal staging using mediastinoscopy. Though most studies have reported a reasonably high negative predictive value (NPV) of FDG PET for mediastinal disease in the region of 90%, invasive mediastinal staging is still recommended due to the failure of PET to detect disease in about 10% cases. Moreover, in regions endemic for infectious and granulomatous disease, there would be more false-positive results leading to a definite fall in specificity and the positive predictive value (PPV) of PET [Figure 9]. Hence, despite positive PET findings, sampling of the mediastinal nodes using invasive mediastinal staging is recommended for histological evidence of N2 disease.[22] Combining the benefits of using both CT and PET in integrated PET/CT, the false-positive results can be reduced. Kim *et al*. improved the specificity

Table 1: General outline for staging based therapy in NSCLC ^

Post staging with PET/CT, MRI brain and invasive mediastinal staging, stage-based treatment regimen					
Stage	Early localized (T1-3, N0-2)			Locoregionally advanced (T4, N3)	Metastatic disease (any T, any N, M1#)
	<N2	N2*	N3		
Therapy	Lung resection with systemic mediastinal nodal dissection	Neo-adjuvant chemotherapy followed by resection	Concurrent chemo-radiation	Concurrent chemo-radiation therapy	Palliative chemotherapy, targeted therapy For brain or symptomatic bone metastases, palliative brain radiation and treatment for bone pain palliation

*Bulky multistation N2 nodes on CT or PET can be directly treated as locoregionally advanced disease with chemoradiation, #Highly selected cases of solitary brain and adrenal metastasis can benefit from resection of metastasis along with resection for lung primary, ^The principles of treatment are not rigid and may vary across institutions depending on availability of resources and expertise

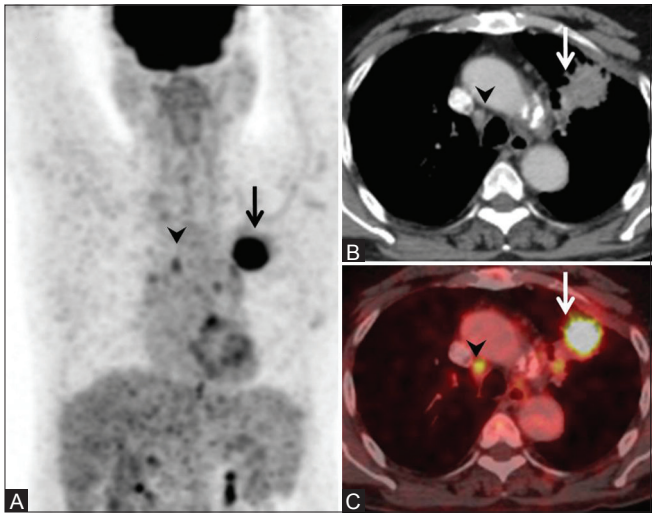

Figure 8 (A-C): FDG PET in nodal disease. Maximum intensity projection (MIP) image shows an FDG-avid primary lung tumor on the left side (arrow, A) and a focus of FDG uptake in the mediastinum (arrowhead, A). CT scan shows enhancing, spiculated primary tumor (arrow, B) and a small right paratracheal node (arrowhead, B) which is negative by size criteria. Fused PET/CT image shows FDG concentration in the primary (arrow, C) as well as the node (arrowhead, C), suggesting metastatic involvement. Mediastinoscopy and biospy revealed metastatic node-N3 disease

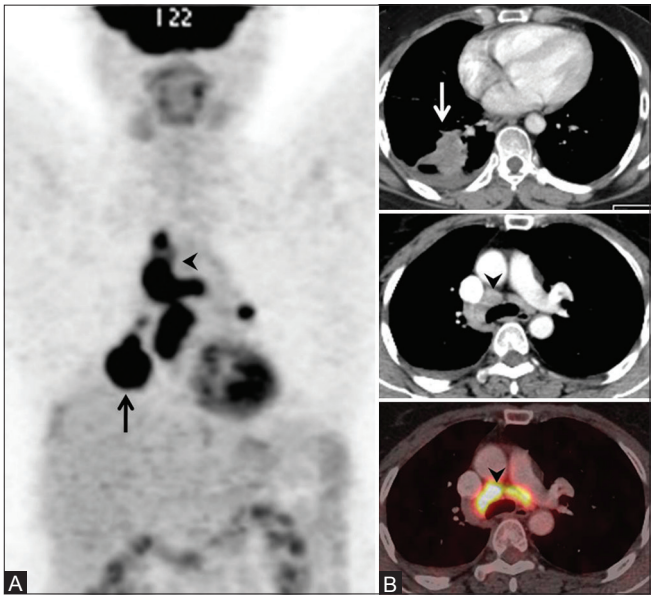

Figure 9 (A and B): FDG PET in nodal disease false-positive study. Maximum intensity projection (MIP) image shows an FDG-avid primary lung tumor on the right side (arrow, A) and multiple foci of FDG uptake in the mediastinum (arrowhead, A). CT scan shows enhancing, primary tumor (arrow, B). Fused PET/CT image shows FDG concentration in the mediastinal nodes, suggesting metastatic involvement. Mediastinoscopy and biospy revealed tuberculosis

of PET/CT by considering nodes which showed obvious calcification or high attenuation [Hounsfield units (HU) >70] on CT scan as benign despite a high FDG uptake in the nodes.[23]

M (metastasis) descriptor

More than half of lung cancer patients have metastatic disease at presentation. Bones, adrenals, brain, and liver are the common distant metastatic sites. Metastatic disease with a few exceptions is not amenable to surgical resection or any kind of potentially curative therapy [Table 1]. Metastatic disease is further sub-classified as M1a or intrathoracic metastasis and M1b or extrathoracic metastasis. This is done due to differences in prognosis between the two categories with M1a having better prognosis than M1b. Malignant pleural effusion, pleural metastases, pericardial disease, and pulmonary nodules in the contralateral lung constitute M1a disease [Figure 10]. M1b disease includes spread to brain, bones, adrenals, liver, and any other distant extra-thoracic site [Figure 10]. Patients with pleural effusions, pericardial disease, and contralateral lung metastases are considered as M1a in the current TNM edition instead of stage T4, since they have a much worse 5-year survival (2-3%) as compared to other T4 tumors (15%) with similar nodal disease burden.[5]

Imaging Modalities for M Stage and Implications of Radiological Findings on Treatment

Intrathoracic metastases (M1a) can be detected on CT scan with a degree of certainty. No additional imaging is required to detect pleural and pericardial effusions and metastatic lung nodules. Adrenal metastases (M1b) are common and detection rate can be as high as 20% at presentation.[24,25] The scan coverage while performing CT scan of the chest should always include the adrenal glands. Detection and confirmation of adrenal involvement is very important, because improved survival has been reported with resection of isolated adrenal metastasis in an otherwise operable lung cancer.[26] Adrenal adenomas are not infrequently seen in the general population and can be confused as metastatic lesions. Demonstration of fat in the adrenal lesion is a highly specific sign of benignancy [Figure 11]. If the adrenal nodule has an HU value of less than 10 on an unenhanced CT scan, then it is highly suggestive of an adenoma with a specificity of 96% and for HU values <0, the specificity increases to 100%.[27-29] Thus, although an HU value <10 is diagnostic of an adenoma, an HU value of greater than 10 is not diagnostic of a metastasis. Thus, an adrenal lesion with HU value >10 at nonenhanced CT can be either an adenoma or metastasis. Other methods like dynamic contrast-enhanced CT scan[30] have been used where >50% contrast washout on delayed imaging is indicative of an adenoma. Chemical shift imaging on MRI using in and opposed phase sequences[31,32] has also been used to characterize adrenal lesions in lung cancer. Thirty percent adenomas can be lipid poor[29,30] and techniques which rely on demonstration of lipid in the adrenal lesion will not be useful in differentiating adenomas from metastases. PET using FDG has been used to characterize indeterminate adrenal lesions. It shows a high sensitivity (97%) and specificity (91%) in differentiating between benign and malignant adrenal lesions [Figure 11] in extra-adrenal malignancies.[33] Though there are several reports which state the use of a quantitative parameter like the Standardized Uptake Value (SUV) cut-off, visual or qualitative assessment of FDG uptake in the adrenal lesion has been found to more useful.[33]

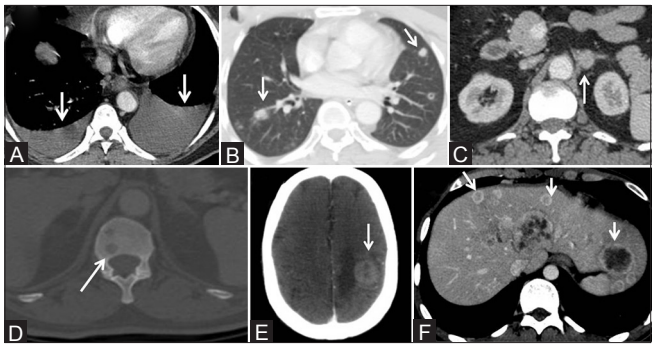

Figure 10 (A-F): Metastatic disease. Bilateral pleural effusions-M1a (arrow, A), lung metastases-M1a (arrows, B), adrenal metastasis-M1b (arrow, C), vertebral metastasis-M1b (arrow, D), brain metastasis-M1b (arrow, E), liver metastases-M1b (arrows, F)

Almost 18% of NSCLC patients will harbor brain metastases.[34,35] MRI is considered to be superior to CT scan in evaluation of brain metastases. Due to an inherently better contrast resolution, lack of bone artifacts, and direct multiplanar imaging, MRI detects more number of lesions and smaller lesions as compared to CT scan[36,37] [Figure 12].

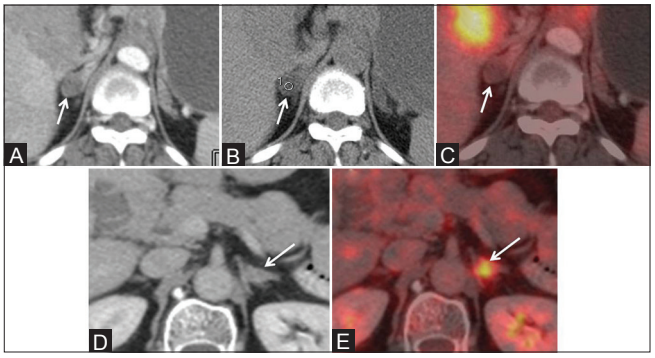

Figure 11 (A-E): Adrenal adenoma versus metastasis. Enhancing solid adrenal nodule on CT scan in a case of lung cancer (arrow, A) suggestive of metastatic deposit. Unenhanced CT scan shows fatty attenuation within the nodule with an HU value of 0 suggesting the possibility of an adenoma (arrow, B). FDG PET/CT shows no tracer concentration in the nodule, confirming the diagnosis of adenoma. Enhancing solid adrenal nodule on CT scan in another patient of lung cancer (arrow, D), which is indeterminate in nature. FDG PET/CT shows abnormal focal tracer concentration in the nodule (arrow, E) highly suggestive of a metastatic deposit

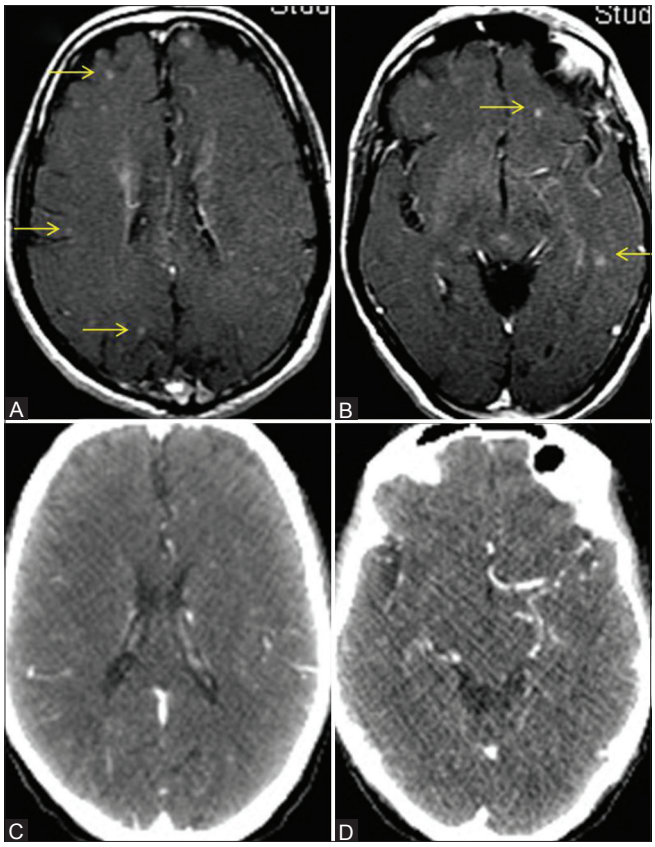

Figure 12 (A-D): Brain metastases in asymptomatic patient, CT scan versus MRI. MRI brain in a patient of lung cancer shows multiple tiny enhancing foci scattered in the parenchyma bilaterally (arrows in A and B) suggestive of metastatic lesions. Corresponding contrast CT scan sections of the brain show no obvious lesions (C and D). Note the beam hardening effects due to bone, leading to a loss of resolution on the CT images (C and D)

MRI is better at detecting metastases in the posterior fossa and the meninges, where CT scan has limitations. In an asymptomatic patient, MRI is more likely to detect brain metastases as compared to CT scan.[38] However, in a patient with neurological signs and symptoms, the difference between sensitivity of MRI and CT scan is less pronounced. Up to 20% patients with solitary brain metastasis on CT scan will harbor multiple lesions on MRI.[36] This observation is clinically relevant because resection of solitary brain metastasis in NSCLC patients is supposed to offer survival advantage[39] [Table 1]. It also has an impact on the type of radiation delivered to the brain – stereotactic radiation for solitary versus whole brain radiation for multiple metastases. The role of FDG PET in the detection of brain metastasis is limited owing to its low sensitivity[40] particularly for small-sized lesions (<1 cm), and thus, its use is restricted in this clinical situation. Even after the integrated use of CECT and PET, MRI is still superior in the diagnosis of brain metastases. Even if the PET/CT study for brain metastases shows negative results, dedicated brain imaging preferably with MRI is essential.

Patients with skeletal metastases present with features of pain or have a laboratory evidence of skeletal disease. Conventionally, skeletal metastases have been evaluated by technetium 99m methylene diphosphonate bone scintigraphy (99m Tc MDP). It is a highly sensitive technique which can detect a lesion much earlier than a radiograph and gives a skeletal map of the entire body from head to toe. However, it is non-specific and false-positive results are seen due to variety of degenerative, infective, and other benign conditions. Hence, a positive bone scan finding has to be confirmed by a more definitive radiological investigation like MRI or CT scan. FDG PET/CT for detection of skeletal metastases performs better than bone scintigraphy. A recent meta-analysis shows that PET/CT has a higher sensitivity and specificity (92% and 98%, respectively) as compared to bone scintigraphy (86% and 87%, respectively) for diagnosing bone metastases.[41] The superiority of PET over bone scans is primarily because of its ability to detect both osteolytic and sclerotic metastases unlike bone scan which has a good sensitivity for detecting sclerotic lesions but slightly underperforms in cases of pure osteolytic disease. Moreover, it has been found that PET is excellent in detecting asymptomatic marrow metastases which can be seen in up to 13% cases of lung cancer[42] [Figure 13].

Presence of pleural effusion is considered as metastatic disease (M1a). When enhancing pleural nodules are seen, the effusion can be attributed to malignant pleural involvement. However, in the absence of enhancing pleural deposits, it is difficult to establish the cause of the effusion. FDG PET can help in characterizing pleural disease by demonstrate tracer uptake in the pleura and is shown to have a high sensitivity and NPV for detecting pleural malignancy[43] [Figure 14]. Challenges can arise in determining the cause of effusion as pleural fluid cytology is positive in only about two-third of cases. In the absence of a positive cytology, if the effusion is large, it is considered to be due to metastatic disease. A thin sliver of fluid from which obtaining cytological confirmation is difficult is assumed to be due to benign pleural reaction, particularly when the tumor is in anatomical contact with the pleura.

Overall Impact of FDG PET/CT on Lung Cancer Staging

FDG PET/CT is now accepted as the standard procedure in the initial staging and diagnostic work-up of lung cancer patients. There is robust evidence in literature in the form of randomized controlled trials which state that addition of FDG PET to the diagnostic work-up reduces the frequency of futile thoracotomies by 20%.[44,45] The primary reason for this is its ability to unmask sites of asymptomatic distant metastatic disease, which makes the patient unsuitable for curative treatment [Figure 15].

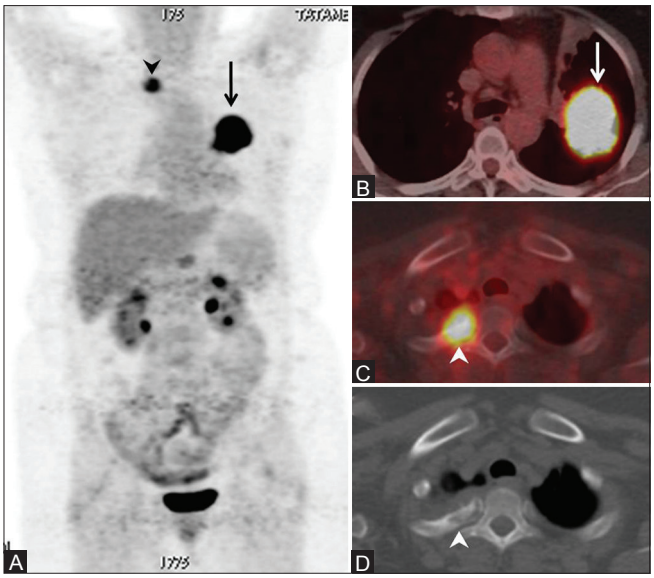

Figure 13 (A-D): Asymptomatic marrow metastases detected on FDG PET/CT. MIP image of an FDG PET scan of a lung cancer patient shows intense tracer concentration in a mass lesion in the left hemithorax (arrows in A and B) and another smaller lesion in the right hemithorax (arrowhead, B). Intense tracer concentration is seen on FDG PET/CT in the right second rib suggesting metastatic disease (arrowhead, C). Note the subtle marrow changes in the rib on CT scan (arrowhead, D)

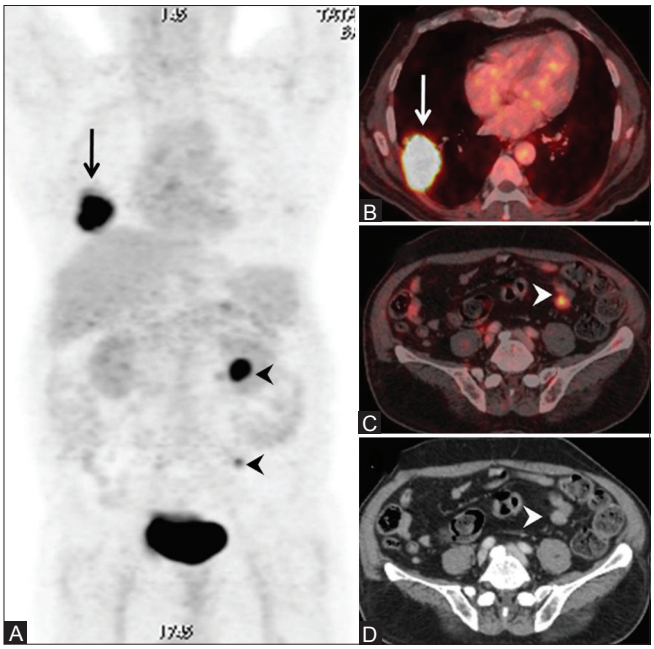

Figure 15 (A-D): Incremental value of FDG PET/CT in baseline staging. MIP image of FDG PET scan shows intense tracer concentration in the right hemithorax (arrow, A) corresponding to a right lung mass (arrow, B). Also seen are two FDG-avid foci in the abdomen (arrowheads, A) which correspond to peritoneal metastatic deposits (arrowhead, C). Note that the peritoneal deposit is almost indistinguishable from adjacent bowel (arrowhead, D). Due to PET/CT findings, the intent of treatment changes from curative surgery of a resectable mass to palliative chemotherapy

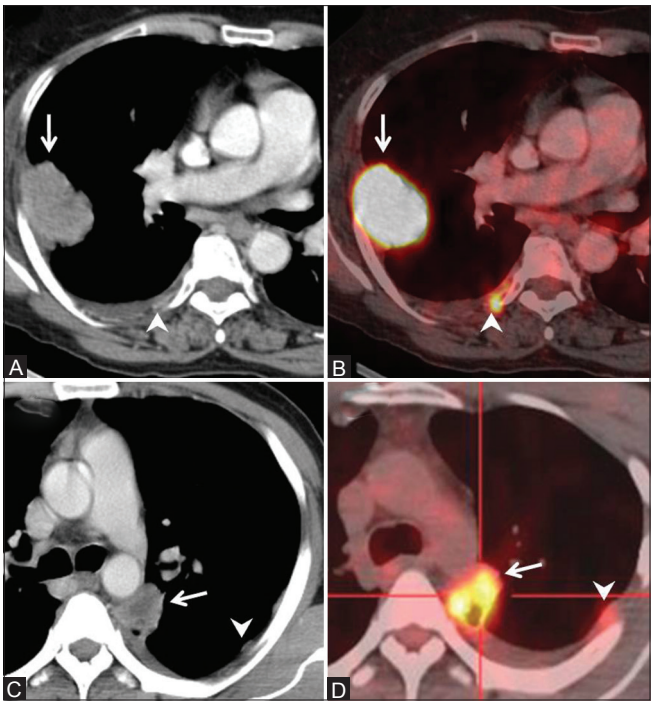

Figure 14 (A-D): Pleural effusion and role of FDG PET/CT. Enhancing lung masses seen on CT scans in two different patients (arrows in A and C) with minimal pleural effusions (arrowheads in A and C). Corresponding PET/CT scans show intense FDG-avid metastatic pleural deposits (arrowheads in B and D) as the cause of effusions. Note that the pleural deposits are barely perceptible on CT

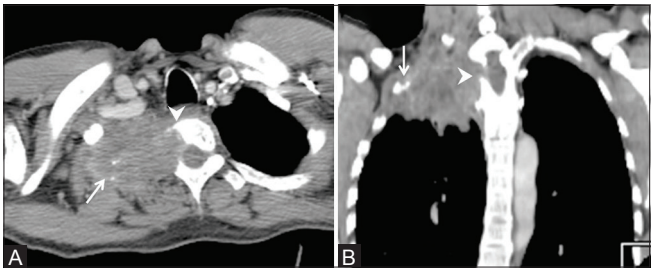

Figure 16 (A and B): Superior sulcus tumor. Axial (A) and coronal (B) CT scans show a large mass in the apex of the right lung causing destruction of the first and second ribs (arrows) with erosion of the right half of the vertebral body (arrowheads) suggestive of a superior sulcus tumor

Addition of intravenous (IV) contrast to integrated PET/CT protocols provides comprehensive staging information for the primary site (T stage), nodes (N stage), and distant disease (M stage). However, it must be borne in mind that FDG PET has a limited ability to detect brain metastases and dedicated brain imaging using MRI is required to rule out brain lesions before a potentially curative treatment is planned. Thus, a combination of PET/CT (with IV contrast) and MRI brain has become a standard practice in staging work-up of lung cancer in several centers.

Superior Sulcus/Pancoast Tumors

They are NSCLCs that arise from the lung apex and invade the chest wall or the soft tissues of the thoracic inlet. They cause clinical signs and symptoms, which together are called Pancoast syndrome. The clinical manifestations include pain in the arm or around the shoulder girdle and Horner's syndrome. Pancoast tumors can be stage T3 or T4. Limited involvement of the chest wall and the lower roots of the brachial plexus (C8 and T1) constitutes T3 stage, whereas extensive involvement including infiltration of C5-C7 nerve roots, esophagus, vertebral body, trachea, and subclavian vessels constitutes T4 disease. Potentially operable tumors are treated with surgery in combination with pre- or postoperative radiation and chemotherapy. Surgery is not performed for tumors that involve the trachea, esophagus, more than 50% of vertebral body, subclavian vessels, and brachial plexus above T1 nerve root.[46-47] N2-N3 nodal involvement and presence of distant metastases also preclude surgery. Thus, accurate and high-resolution imaging is necessary to delineate various structures in a crowded and narrow region like the superior sulcus. CT scan is excellent for detection of rib and vertebral erosion as well as for vascular invasion [Figure 16]. However, MRI with its multiplanar capability and higher contrast resolution is used to diagnose involvement of the brachial plexus and extension to the neural foramina and the spinal canal.

Small Cell Cancer

Small cell lung cancers (SCLCs) account for about 13-15% of lung malignancies and are seen almost exclusively in smokers. SCLCs are very aggressive tumors known for their high growth rate and early development of metastatic disease. Majority of these tumors present with advanced or metastatic disease and in spite of initial response to treatment, they show worse long-term survival than NSCLC.[48] On imaging, they present with bulky mediastinal nodes which conglomerate to form a large mass. The primary tumor is often not visualized as a discrete entity as in NSCLC and appears to merge with the nodal disease [Figure 17]. Previously, SCLC was divided into two categories: limited disease and extensive disease. Tumor along with its nodal disease confined to one hemithorax which could be covered in a single radiation field was classified as limited disease. Extensive disease included extrathoracic disease and distant metastases. Currently, SCLCs are staged with the same TNM descriptors as NSCLC, though treatment decisions are still made by classifying the disease as limited or extensive stage.

Dynamic Perfusion Imaging in Lung Cancer

Advanced CT techniques like dynamic perfusion imaging have been used in lung cancer to study the tumor angiogenesis. This technique correlates well with micro-vessel density and expression of vascular endothelial growth factor which reflect tumor angiogenesis.[49] This has important implications in planning and assessing response to anti-angiogenic therapy.

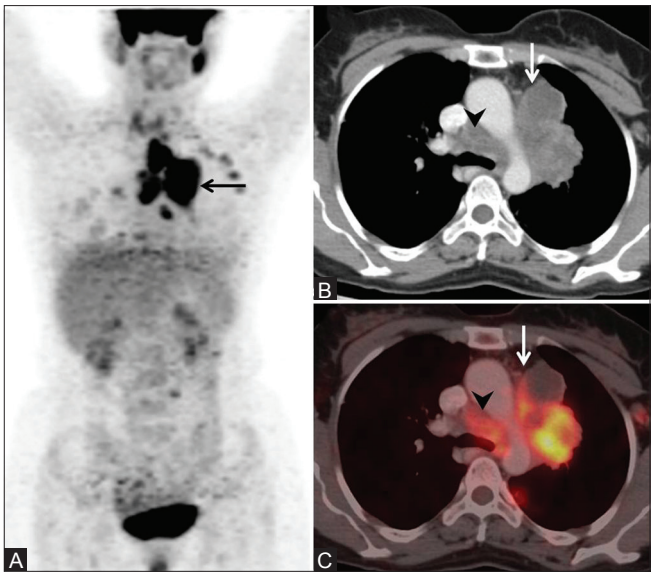

Figure 17 (A-C): Small cell lung cancer (limited stage). MIP image of an FDG PET study shows intense tracer concentration in the mediastinum (arrow, A) which corresponds to an FDG-avid soft tissue mass on CT and PET/CT (arrow in B and C) which extends into the mediastinum and appears to conglomerate and merge with the nodal disease (arrowheads, B). This is a typical radiological appearance of small cell cancers. No extrathoracic metastatic site is seen on the MIP image (A)

Conclusion

Radiologists play a critical role in the multidisciplinary management of lung cancer patients. In addition to accurately describing the radiological extent of the disease, it is important to understand the principles of staging, the clinical relevance of various radiological staging descriptors, and their impact on treatment decisions.

References

1. Mountain CF. Revisions in the international system for staging lung cancer. Chest 1997;111:1710-7.
2. Ferlay J, Soerjomataram I, Ervik M, Dikshit R, Eser S, Mathers C, *et al*. GLOBOCAN 2012 v1.0, Cancer Incidence and Mortality Worldwide: IARC CancerBase No. 11.Lyon, France: International Agency for Research on Cancer, 2013. Available from: http://www.globocan.iarc.fr. [Last accessed on 2014 Jun 15].
3. Buccheri G, Ferrigno D. Lung cancer: Clinical presentation and specialist referral time. Eur Respir J 2004;24:898-904.
4. American Cancer Society. Cancer facts and figures 2008. Atlanta, Ga: American Cancer Society; 2008.
5. Goldstraw P, Crowley J, Chansky K, Giroux DJ, Groome PA, Rami-Porta R, *et al*. The IASLC lung cancer staging project: Proposals for the revision of the TNM stage groupings in the forthcoming (seventh) edition of the TNM classification of malignant tumours. J Thorac Oncol 2007;2:706-14.
6. Rami-Porta R, Ball D, Crowley J, Giroux DJ, Jett J, Travis WD, *et al*. The IASLC Lung Cancer Staging Project: Proposals for the revision

of the T descriptors in the forthcoming (seventh) edition of the TNM classification for lung cancer. J Thorac Oncol 2007;2:593-602.
7. Quint LE, Francis IR. Radiologic staging of lung cancer. J Thorac Imaging 1999;14:235-46.
8. Padovani B, Mouroux J, Seksik L, Chanalet S, Sedat J, Rotomondo C, *et al*. Chest wall invasion by bronchogenic carcinoma: Evaluation with MR imaging. Radiology 1993;187:33-8.
9. Webb WR, Gatsonis C, Zerhouni EA, Heelan RT, Glazer GM, Francis IR, *et al*. CT and MR imaging in staging non–small cell bronchogenic carcinoma: Report of the radiologic diagnostic oncology group. Radiology 1991;178:705-13.
10. Glazer HS, Duncan-Meyer J, Aronberg DJ, Moran JF, Levitt RG, Sagel SS. Pleural and chest wall invasion in bronchogenic carcinoma: CT evaluation. Radiology 1985;157:191-4.
11. van Baardwijk A, Baumert BG, Bosmans G, van Kroonenburgh M, Stroobants S, Gregoire V, *et al*. The current status of FDG-PET in tumour volume definition in radiotherapy treatment planning. Cancer Treat Rev 2006;32:245-60.
12. Purandare NC, Kulkarni AV, Kulkarni SS, Roy D, Agrawal A, Shah S, *et al*. 18F-FDG PET/CT-directed biopsy: Does it offer incremental benefit? Nucl Med Commun 2013;34:203-10.
13. Mountain CF, Dresler CM. Regional lymph node classification for lung cancer staging. Chest 1997;111:1718-23.
14. Naruke T, Suemasu K, Ishikawa S. Lymph node mapping and curability at various levels of metastasis in resected lung cancer. J Thorac Cardiovasc Surg 1978;76:832-9.
15. Rusch VW, Asamura H, Watanabe H, Giroux DJ, Rami-Porta R, Goldstraw P, *et al*. The IASLC lung cancer staging project: A proposal for a new international lymph node map in the forthcoming seventh edition of the TNM classification for lung cancer. J Thorac Oncol 2009;4:568-77.
16. Rosell R, Gómez-Codina J, Camps C, Maestre J, Padille J, Cantó A, *et al*. A randomized trial comparing preoperative chemotherapy plus surgery with surgery alone in patients with non-small-cell lung cancer. N Engl J Med 1994;330:153-8.
17. Aupérin A, Le Péchoux C, Rolland E, Curran WJ, Furuse K, Fournel P, *et al*. Meta-analysis of concomitant versus sequential radiochemotherapy in locally advanced non-small-cell lung cancer. J Clin Oncol 2010;28:2181-90.
18. Dales RE, Stark RM, Raman S. Computed tomography to stage lung cancer. Approaching a controversy using meta-analysis. Am Rev Respir Dis 1990;141:1096-101.
19. Dwamena BA, Sonnad SS, Angobaldo JO, Wahl RL. Metastases from non-small cell lung cancer: Mediastinal staging in the 1990s--meta-analytic comparison of PET and CT. Radiology 1999;213:530-6.
20. Ikezoe J, Kadowaki K, Morimoto S, Takashima S, Kozuka T, Nakahara K, *et al*. Mediastinal lymph node metastases from nonsmall cell bronchogenic carcinoma: Reevaluation with CT. J Comput Assist Tomogr 1990;14:340-4.
21. Wu Y, Li P, Zhang H, Shi Y, Wu H, Zhang J, *et al*. Diagnostic value of fluorine 18 fluorodeoxyglucose positron emission tomography/computed tomography for the detection of metastases in non-small-cell lung cancer patients. Int J Cancer 2013;132:E37-47.
22. De Leyn P, Lardinois D, Van Schil PE, Rami-Porta R, Passlick B, Zielinski M, *et al*. ESTS guidelines for preoperative lymph node staging for non-small cell lung cancer. Eur J Cardiothorac Surg 2007;32:1-8.
23. Kim YK, Lee KS, Kim BT, Choi JY, Kim H, Kwon OJ, *et al*. Mediastinal nodal staging of nonsmall cell lung cancer using integrated 18F-FDG PET/CT in a tuberculosis-endemic country: Diagnostic efficacy in 674 patients. Cancer 2007;109:1068-77.
24. Nielsen ME Jr, Heaston DK, Dunnick NR, Korobkin M. Preoperative CT evaluation of adrenal glands in non-small cell bronchogenic carcinoma. AJR Am J Roentgenol 1982;139:317-20.
25. Pagani JJ. Non-small cell lung carcinoma adrenal metastases. Computed tomography and percutaneous needle biopsy in their diagnosis. Cancer 1984;53:1058-60.
26. Porte H, Siat J, Guibert B, Lepimpec-Barthes F, Jancovici R, Bernard A, *et al*. Resection of adrenal metastases from non-small cell lung cancer: A multicenter study. Ann Thorac Surg 2001;71:981-5.
27. Boland GW, Lee MJ, Gazelle GS, Halpern EF, McNicholas MM, Mueller PR. Characterization of adrenal masses using unenhanced CT: An analysis of the CT literature. AJR Am J Roentgenol 1998;171:201-4.
28. Korobkin M, Brodeur FJ, Yutzy GG, Francis IR, Quint LE, Dunnick NR, *et al*. Differentiation of adrenal adenomas from nonadenomas using CT attenuation values. AJR Am J Roentgenol 1996;166:531-6.
29. Caoili EM, Korobkin M, Francis IR, Cohan RH, Dunnick NR. Delayed enhanced CT of lipid-poor adrenal adenomas. AJR Am J Roentgenol 2000;175:1411-5.
30. Peña CS, Boland GW, Hahn PF, Lee MJ, Mueller PR. Characterization of indeterminate (lipid-poor) adrenal masses: Use of washout characteristics at contrast-enhanced CT. Radiology 2000;217:798-802.
31. Mitchell DG, Crovello M, Matteucci T, Petersen RO, Miettinen MM. Benign adrenocortical masses: Diagnosis with chemical shift MR imaging. Radiology 1992;185:345-51.
32. Reinig JW, Stutley JE, Leonhurdt CM, Spicer KM, Margolis M, Caldwell CB. Differentiation of adrenal masses with MR imaging: Comparison of techniques. Radiology 1994;192:41-6.
33. Boland GW, Dwamena BA, Jagtiani Sangwaiya M, Goehler AG, Blake MA, Hahn PF, *et al*. Characterization of adrenal masses by using FDG PET: A systematic review and meta-analysis of diagnostic test performance. Radiology 2011;259:117-26.
34. Wong J, Haramati LB, Rozenshtein A, Yanez M, Austin JH. Non-small-cell lung cancer: Practice patterns of extrathoracic imaging. Acad Radiol 1999;6:211-5.
35. Mintz BJ, Tuhrim S, Alexander S, Yang WC, Shanzer S. Intracranial metastases in the initial staging of bronchogenic carcinoma. Chest 1984;86:850-3.
36. Schellinger PD, Meinck HM, Thron A. Diagnostic accuracy of MRI compared to CCT in patients with brain metastases. J Neurooncol 1999;44:275-81.
37. Suzuki K, Yamamoto M, Hasegawa Y, Ando M, Shima K, Sako C, *et al*. Magnetic resonance imaging and computed tomography in the diagnoses of brain metastases of lung cancer. Lung Cancer 2004;46:357-60.
38. Yokoi K, Kamiya N, Matsuguma H, Machida S, Hirose T, Mori K, *et al*. Detection of brain metastasis in potentially operable non-small cell lung cancer: A comparison of CT and MRI. Chest 1999;115:714-9.
39. Billing PS, Miller DL, Allen MS, Deschamps C, Trastek VF, Pairolero PC. Surgical treatment of primary lung cancer with synchronous brain metastases. J Thorac Cardiovasc Surg 2001;122:548-53.
40. Ludwig V, Komori T, Kolb D, Martin WH, Sandler MP, Delbeke D. Cerebral lesions incidentally detected on 2-deoxy-2-[18F] fluoro-D-glucose positron emission tomography images of patients evaluated for body malignancies. Mol Imaging Biol 2002;4:359-62.
41. Qu X, Huang X, Yan W, Wu L, Dai K. A meta-analysis of ^{18}FDG-PET-CT, ^{18}FDG-PET, MRI and bone scintigraphy for diagnosis of bone metastases in patients with lung cancer. Eur J Radiol 2012;81:1007-15.
42. Bury T, Barreto A, Daenen F, Barthelemy N, Ghaye B, Rigo P. Fluorine-18 deoxyglucose positron emission tomography for the detection of bone metastases in patients with non-small cell lung cancer. Eur J Nucl Med 1998;25:1244-7.

43. Schaffler GJ, Wolf G, Schoellnast H, Groell R, Maier A, Smolle-Jüttner FM, *et al*. Non-small cell lung cancer: Evaluation of pleural abnormalities on CT scans with 18F FDG PET. Radiology 2004;231:858-65.
44. van Tinteren H, Hoekstra OS, Smit EF, van den Bergh JH, Schreurs AJ, Stallaert RA, *et al*. Effectiveness of positron emission tomography in the preoperative assessment of patients with suspected non-small-cell lung cancer: The PLUS multicentre randomised trial. Lancet 2002;359:1388-93.
45. Fischer B, Lassen U, Mortensen J, Larsen S, Loft A, Bertelsen A, *et al*. Preoperative staging of lung cancer with combined PET-CT. N Engl J Med 2009;361:32-9.
46. Bilsky MH, Vitaz TW, Boland PJ, Bains MS, Rajaraman V, Rusch VW. Surgical treatment of superior sulcus tumors with spinal and brachial plexus involvement. J Neurosurg 2002;97(Suppl):301-9.
47. Dartevelle P, Macchiarini P. Surgical management of superior sulcus tumors. Oncologist 1999;4:398-407.
48. Sher T, Dy GK, Adjei AA. Small cell lung cancer. Mayo Clin Proc 2008;83:355-67.
49. Ma SH, Le HB, Jia BH, Wang ZX, Xiao ZW, Cheng XL, *et al*. Peripheral pulmonary nodules: Relationship between multi-slice spiral CT perfusion imaging and tumor angiogenesis and VEGF expression. BMC Cancer 2008;8:186.

Cite this article as: Purandare NC, Rangarajan V. Imaging of lung cancer: Implications on staging and management. Indian J Radiol Imaging 2015;25:109-20.

Source of Support: Nil, **Conflict of Interest:** None declared.